Available online at www.sciencedirect.com

ScienceDirect

Ceramics International 40 (2014) 3511–3516

CERAMICS INTERNATIONAL

www.elsevier.com/locate/ceramint

Electrochemical characteristics of $LiNi_{0.7}Co_{0.3}O_2$ synthesized at 850 °C from carbonates or oxides of Li, Ni, and Co

Ho Rim[a,*], Jiyoung Song[b,c], Daniel R. Mumm[c]

[a]ASE Korea, 494 Munbal-dong Paju-si Gyeonggi-do, 413-790, Republic of Korea
[b]Woodbridge High School, 2 Meadowbrook Irvine, CA 92604, USA
[c]Department of Chemical Engineering and Materials Science, University of California Irvine, Irvine, CA 92697-2575, USA

Received 20 August 2013; accepted 17 September 2013
Available online 25 September 2013

Abstract

Cathode active materials with a composition of $LiNi_{0.7}Co_{0.3}O_2$ were synthesized by a solid-state reaction method at 850 °C using Li_2CO_3, NiO or $NiCO_3$, and Co_3O_4 or $CoCO_3$ as the sources of Li, Ni, and Co, respectively. Electrochemical properties, structure, and microstructure of the synthesized $LiNi_{0.7}Co_{0.3}O_2$ samples were analyzed. The curves of voltage vs. x in $Li_xNi_{0.7}Co_{0.3}O_2$ for the first charge–discharge and the intercalated and deintercalated Li quantity Δx were studied. The $LiNi_{0.7}Co_{0.3}O_2$ sample synthesized from Li_2CO_3, NiO, and Co_3O_4 had the largest first discharge capacity (127 mAh/g), with a discharge capacity deterioration rate of 2.9 mAh/g/cycle. The $LiNi_{0.7}Co_{0.3}O_2$ sample synthesized from Li_2CO_3, $NiCO_3$, and Co_3O_4 had the smallest capacity deterioration rate of 1.3 mAh/g/cycle.

Keywords: $LiNi_{0.7}Co_{0.3}O_2$; Solid-state reaction method; Various starting materials; Curve of voltage vs. x in $Li_xNi_{0.7}Co_{0.3}O_2$; Discharge capacity

1. Introduction

Lithium secondary battery is one of the most interesting types of rechargeable battery for portable electronics. It has quite high energy densities, no memory effect, and only a slow self-discharge loss. Interest is also growing in using the lithium secondary battery for military, electric vehicle, and aerospace applications.

$LiCoO_2$ [1–5], $LiNiO_2$ [6–13], and $LiMn_2O_4$ [14–20] have been studied by many researchers as cathode materials for lithium secondary batteries [21]. $LiMn_2O_4$ contains a relatively inexpensive element, Mn, and is environment-friendly, but its cycling performance is poor. $LiCoO_2$ has a large diffusivity and a high operating voltage, and it can be synthesized relatively easily. However, it has a disadvantage in that it contains an expensive element, Co. $LiNiO_2$ has a large discharge capacity [22], and is relatively excellent economically and environmentally. However, since Li and Ni have similar sizes ($Li^+ = 0.72$ Å and $Ni^{2+} = 0.69$ Å), $LiNiO_2$ is usually obtained in non-stoichiometric compositions, $Li_{1-y}Ni_{1+y}O_2$ [23,24]. The Ni^{2+} ions in the lithium planes obstruct the movement of the $Li+$ ions during intercalation and deintercalation [5–25].

The weaknesses of $LiCoO_2$ and $LiNiO_2$ were overcome by incorporating $LiCoO_2$ and $LiNiO_2$ phases into $LiNi_{1-y}Co_yO_2$ compositions because the presence of cobalt stabilizes the structure in a strictly two-dimensional fashion, thus favoring good reversibility of the intercalation and deintercalation reactions [26–38]. Rougier et al. [26] reported that the stabilization of the two-dimensional character of the structure by cobalt substitution in $LiNiO_2$ is correlated with an increase in the cell performance, due to the decrease in the amount of extra nickel ions in the inter-slab space which impede the lithium diffusion.

To synthesize $LiNi_{1-y}Co_yO_2$ by the solid-state reaction method [26–30,32–34,38–40], different starting materials have been used by researchers. $LiOH \cdot H_2O$ or Li_2CO_3, NiO or $NiCO_3$, and Co_3O_4 or $CoCO_3$ have been used as starting materials by some researchers [40].

In this work, $LiNi_{0.7}Co_{0.3}O_2$ cathode materials were synthesized by a solid-state reaction method at 850 °C using Li_2CO_3, NiO or $NiCO_3$, and Co_3O_4 or $CoCO_3$ as the sources of Li, Ni,

*Corresponding author. Tel.: +82 1 020 847 278; fax: +82 6 327 023 86.
E-mail addresses: highlender@hanmail.net, holender@naver.com (H. Rim).

0272-8842/$ - see front matter © 2013 Elsevier Ltd and Techna Group S.r.l. All rights reserved.
http://dx.doi.org/10.1016/j.ceramint.2013.09.078

and Co, respectively. The electrochemical properties of the synthesized samples were then examined. The structure of the synthesized $LiNi_{0.7}Co_{0.3}O_2$ was analyzed, and the microstructures of the samples were observed. The curves of voltage vs. x in $Li_xNi_{0.7}Co_{0.3}O_2$ for the first charge–discharge and the intercalated and deintercalated Li quantity Δx were studied.

2. Experimental

Li_2CO_3, NiO or $NiCO_3$, and Co_3O_4 or $CoCO_3$ were used as starting materials in order to synthesize $LiNi_{0.7}Co_{0.3}O_2$ by the solid-state reaction method. All the starting materials (with purities of 99.9%) were purchased from Aldrich Co.

Fig. 1 schematically shows the experimental procedure for the synthesis of $LiNi_{0.7}Co_{0.3}O_2$ from Li_2CO_3, NiO or $NiCO_3$, and Co_3O_4 or $CoCO_3$ as the sources of Li, Ni, and Co, respectively, and the characterization of the synthesized samples. The mixture of the starting materials with the composition of $LiNi_{0.7}Co_{0.3}O_2$ was sufficiently mixed and pelletized. The pellet was then heat-treated in air at 650 °C for 20 h. It was then ground, mixed, pelletized, and calcined at 850 °C for 20 h. Then, this pellet was cooled at a rate of 50 °C/min, and then ground, mixed, and pelletized again. Finally, it was calcined again at 850 °C for 20 h.

The phase identification of the synthesized samples was carried out by X-Ray Diffraction (XRD) analysis using Cu K_α radiation (Mac-Science Co., Ltd.). The scanning rate was 16 °/min, and the scanning range of the diffraction angle (2θ) was $10^\circ \leq 2\theta \leq 70^\circ$. The morphologies of the samples were observed using a scanning electron microscope (SEM).

Electrochemical cells consisted of $LiNi_{0.7}Co_{0.3}O_2$ as a positive electrode, Li foil as a negative electrode, and an electrolyte of 1 M $LiPF_6$ in a 1:1 (volume ratio) mixture of ethylene carbonate (EC) and dimethyl carbonate (DMC). Whatman glass-fiber was used as the separator. The cells were assembled in an argon-filled dry box. To fabricate the positive electrode, 89 wt% synthesized oxide, 10 wt% acetylene black, and 1 wt% polytetrafluoroethylene (PTFE) binder were mixed in an agate mortar. By introducing Li metal, Whatman glass-fiber, the positive electrode, and the electrolyte, the cell was assembled. Fig. 2 shows a schematic diagram of the cell used in this work. The current-collectors were stainless-steel screws with a hole at the end to which a copper wire is connected. All the electrochemical tests were performed at room temperature with a potentiostatic/galvanostatic system (Mac-Pile system, Bio-Logic Co. Ltd.). The cells were cycled at a current density of 200 μA/cm^2 in a voltage range of 3.2–4.3 V.

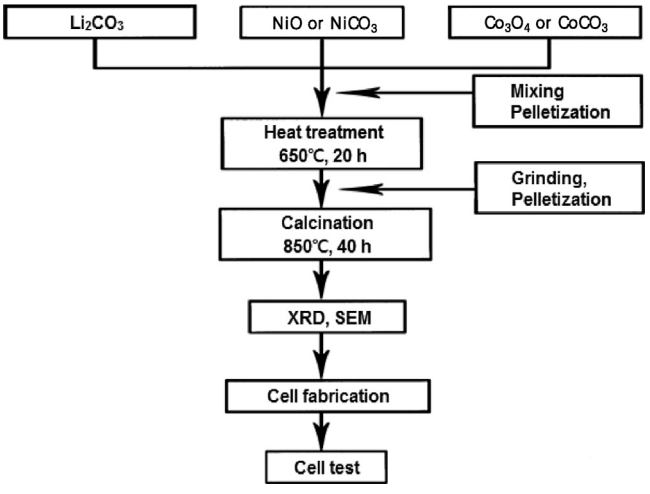

Fig. 1. Experimental procedure for $LiNi_{0.7}Co_{0.3}O_2$ synthesis from Li_2CO_3, NiO or $NiCO_3$, and Co_3O_4 or $CoCO_3$ as the sources of Li, Ni, and Co, respectively, and the characterization of the synthesized $LiNi_{0.7}Co_{0.3}O_2$.

3. Results and discussion

The XRD patterns of the $LiNi_{0.7}Co_{0.3}O_2$ and $LiCoO_2$ powders calcined at 850 °C for 40 h using $LiCO_3$, $NiCO_3$ and $CoCO_3$ as starting materials are shown in Fig. 3. The peaks are identified as corresponding to those of the $LiNiO_2$ phase, which has α-$NaFeO_2$ structure with a space group of $R\bar{3}m$. The fraction of each phase from the intensity ratios of the 003 and 104 peaks can be calculated since the 003 peak originates from the diffraction of only the $R\bar{3}m$ α-$NaFeO_2$ structure while the 104 peak originates from the diffractions of both the $R\bar{3}m$ α-$NaFeO_2$ and $Fm\bar{3}m$ NaCl structures. The

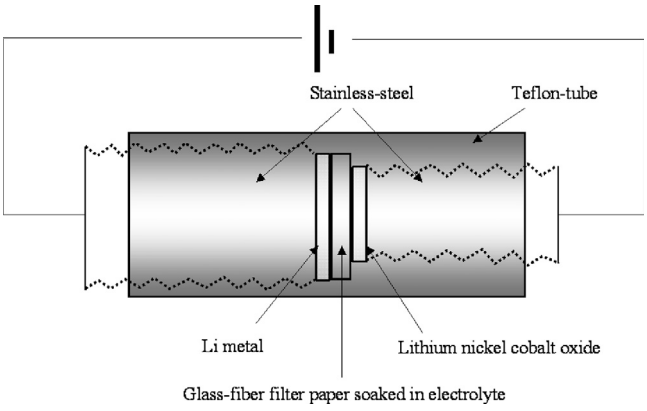

Fig. 2. Schematic diagram of the electrochemical cell used in this work.

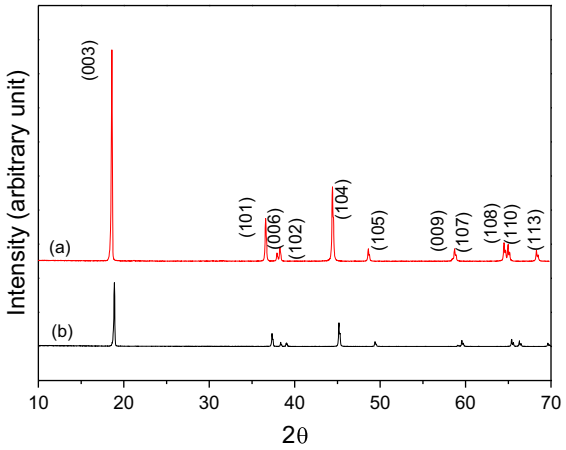

Fig. 3. X-ray (CuK_α) diffraction patterns of (a) $LiNi_{0.7}Co_{0.3}O_2$ and (b) $LiCoO_2$ synthesized from Li_2CO_3, $NiCO_3$ and $CoCO_3$.

value of the intensity ratio of the 003 and 104 peaks, I_{003}/I_{104}, for a completely stoichiometric composition $LiNiO_2$ was reported to be about 1.3 by Morales et al. [24]. Ohzuku et al. [39] reported that, as the intensity ratio of the 003 and 104 peaks increases, the degree of displacement of the nickel and lithium ions decreases. They also reported that electroactive $LiNiO_2$ showed a clear split of the (108) and (110) lines, which appear in their XRD patterns at a diffraction angle near $2\theta = 65^\circ$. The XRD pattern of the $LiNi_{0.7}Co_{0.3}O_2$ powder synthesized using $LiCO_3$, $NiCO_3$, and $CoCO_3$, exhibited in Fig. 3, shows that the intensity ratio of the 003 and 104 peaks is quite high and exhibits a clear split of the (108) and (110) lines.

Fig. 4 shows the SEM micrographs of the $LiNi_{0.7}Co_{0.3}O_2$ synthesized at 850 °C from combinations of starting materials: (a) Li_2CO_3, NiO, and Co_3O_4, (b) Li_2CO_3, $NiCO_3$, and Co_3O_4, and (c) Li_2CO_3, $NiCO_3$, and $CoCO_3$. Overall, the sample (a) has the largest particles, followed in order by sample (c) and sample (b). The surfaces of large particles of sample are flat. The particles of the samples (b) are agglomerated.

The curves of voltage vs. x in $Li_xNi_{0.7}Co_{0.3}O_2$ at a current density of 200 μA/cm^2 are shown in Fig. 5 for the first

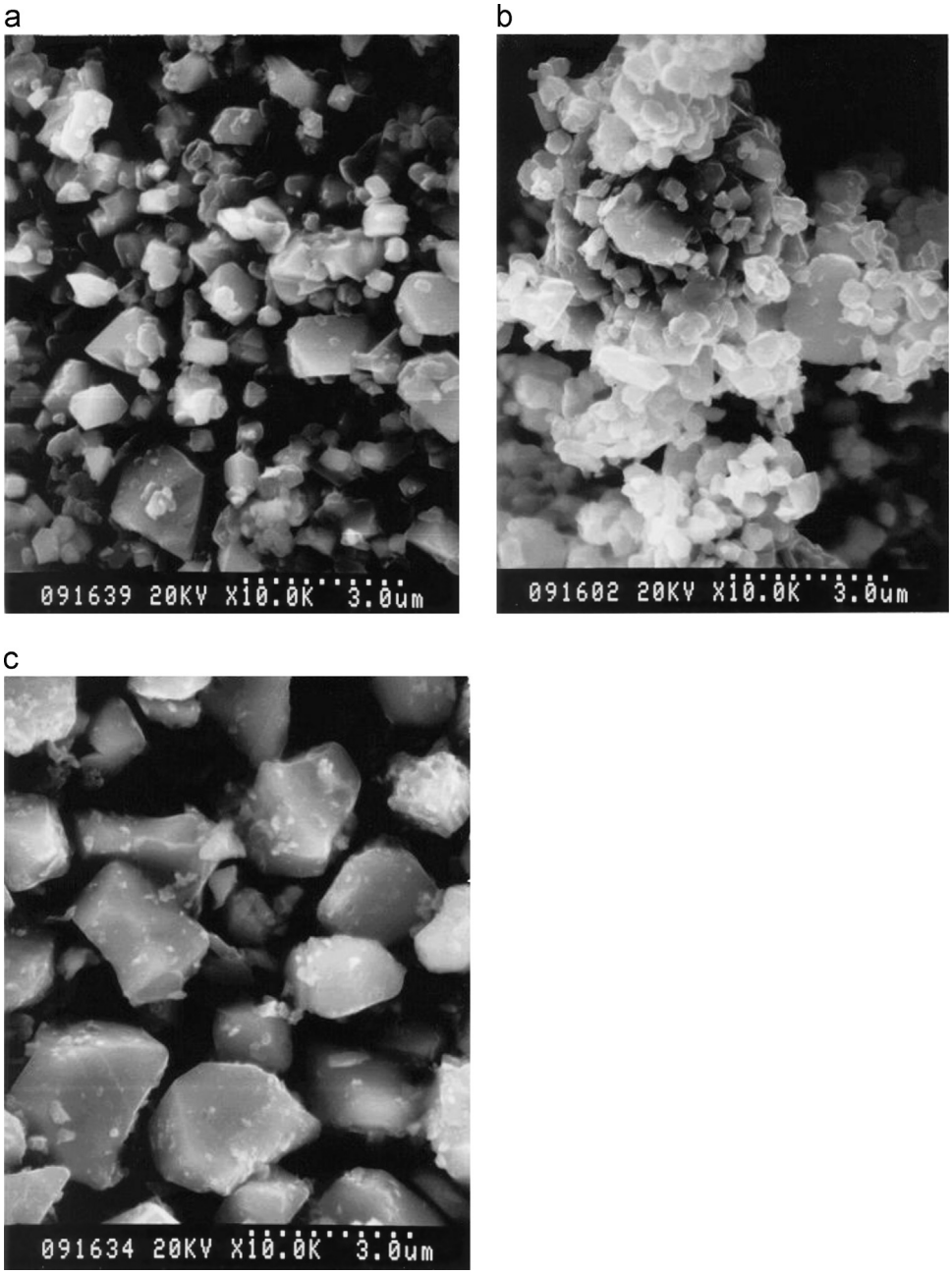

Fig. 4. SEM micrographs of the $LiNi_{0.7}Co_{0.3}O_2$ synthesized at 850 °C from combinations of starting materials: (a) Li_2CO_3, NiO, and Co_3O_4, (b) Li_2CO_3, $NiCO_3$, and Co_3O_4, and (c) Li_2CO_3, $NiCO_3$, and $CoCO_3$.

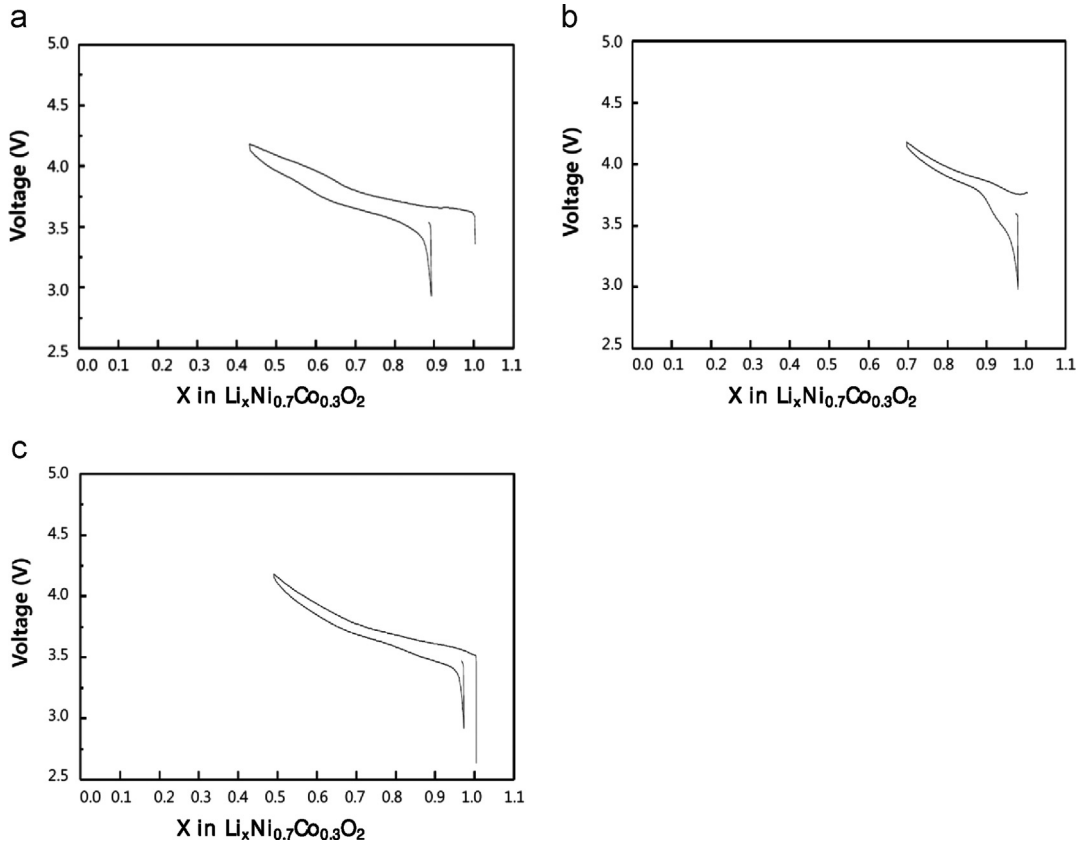

Fig. 5. Curves of voltage vs. x in $Li_xNi_{0.7}Co_{0.3}O_2$ at a current density of 200 μA/cm^2 for the first charge–discharge of $LiNi_{0.7}Co_{0.3}O_2$ synthesized at 850 °C from combinations of starting materials: (a) Li_2CO_3, NiO, and Co_3O_4, (b) Li_2CO_3, $NiCO_3$, and Co_3O_4, and (c) Li_2CO_3, $NiCO_3$, and $CoCO_3$.

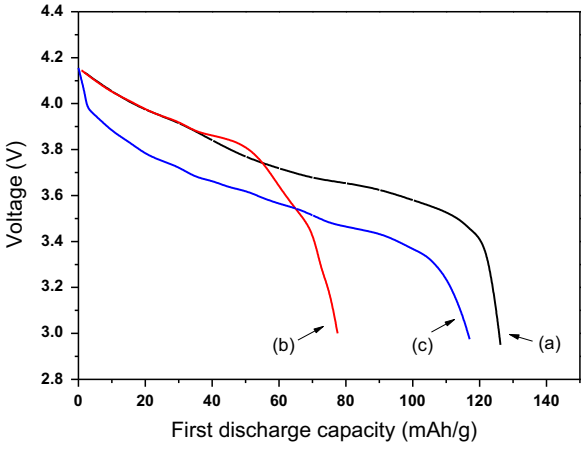

Fig. 6. The first discharge capacities at a current density of 200 μA/cm^2 in the voltage range of 3.0–4.3 V for $LiNi_{0.7}Co_{0.3}O_2$ synthesized at 850 °C from combinations of starting materials: (a) Li_2CO_3, NiO, and Co_3O_4, (b) Li_2CO_3, $NiCO_3$, and Co_3O_4, and (c) Li_2CO_3, $NiCO_3$, and $CoCO_3$.

charge–discharge of $LiNi_{0.7}Co_{0.3}O_2$ synthesized at 850 °C from combinations of starting materials: (a) Li_2CO_3, NiO, and Co_3O_4, (b) Li_2CO_3, $NiCO_3$, and Co_3O_4, and (c) Li_2CO_3, $NiCO_3$, and $CoCO_3$. Polarization is a change in the potentials for the deintercalation and intercalation of lithium atoms. The sample (c) has the smallest polarization, followed in order by sample (b) and sample (a). The charge or discharge capacity is proportional to the value of Δx in $Li_xNi_{0.9}Co_{0.1}O_2$. The sample (a) has the largest discharge capacity, followed in order by sample (c) and sample (b).

The first discharge capacities at a current density of 200 μA/cm^2 in the voltage range of 3.0–4.3 V are shown in Fig. 6 for $LiNi_{0.7}Co_{0.3}O_2$ synthesized at 850 °C from different combinations of starting materials: (a) Li_2CO_3, NiO, and Co_3O_4, (b) Li_2CO_3, $NiCO_3$, and Co_3O_4, and (c) Li_2CO_3, $NiCO_3$, and $CoCO_3$. The curves for the sample (a) and the sample (c) have quite long plateaus. The sample (a) has the largest first discharge capacity, followed in order by the sample (c) and the sample (b).

The variations of the discharge capacity with the number of cycles (n) for $LiNi_{0.7}Co_{0.3}O_2$ synthesized at 850 °C from (a) Li_2CO_3, NiO, and Co_3O_4, (b) Li_2CO_3, $NiCO_3$, and Co_3O_4, and (c) Li_2CO_3, $NiCO_3$, and $CoCO_3$ are shown in Fig. 7. The sample (a) has the largest first discharge capacity (127 mAh/g), followed in order by sample (c) (119 mAh/g), and (b) (78 mAh/g). The sample (a) has the largest particles with quite flat surfaces (Fig. 4). The sample (b) has the best cycling performance, followed in order by the samples (c) and (a).

Fig. 8 shows the variations of the first-discharge capacity and the capacity deterioration rate of the $LiNi_{0.7}Co_{0.3}O_2$ synthesized at 850 °C with the following combinations of starting materials: (a) Li_2CO_3, NiO, and Co_3O_4, (b) Li_2CO_3, $NiCO_3$, and Co_3O_4, and (c) Li_2CO_3, $NiCO_3$, and $CoCO_3$. The sample (a) has the largest first-discharge capacity, followed in order by sample (c) and sample (b). The sample (b) has the smallest capacity

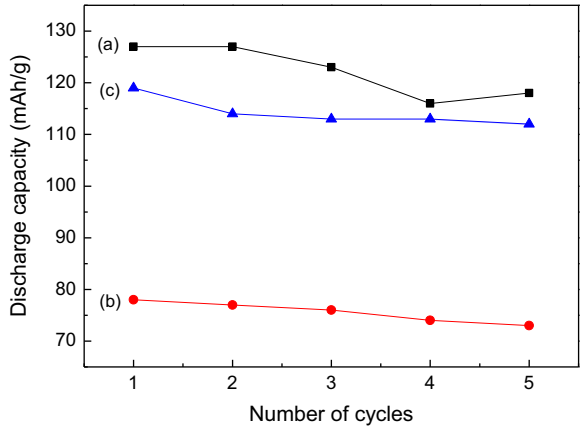

Fig. 7. Variations of the discharge capacity with number of cycles (n) for $LiNi_{0.7}Co_{0.3}O_2$ synthesized at 850 °C from (a) Li_2CO_3, NiO, and Co_3O_4, (b) Li_2CO_3, $NiCO_3$, and Co_3O_4, and (c) Li_2CO_3, $NiCO_3$, and $CoCO_3$.

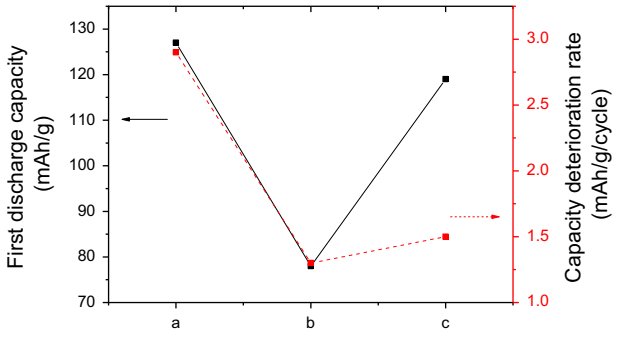

Fig. 8. Variations of the first discharge capacity and the capacity deterioration rate of the $LiNi_{0.7}Co_{0.3}O_2$ synthesized at 850 °C with combinations of starting materials: (a) Li_2CO_3, NiO, and Co_3O_4, (b) Li_2CO_3, $NiCO_3$, and Co_3O_4, and (c) Li_2CO_3, $NiCO_3$, and $CoCO_3$.

deterioration rate (1.3 mAh/g/cycle), followed in order by sample (c) (1.5 mAh/g/cycle), and sample (a) (2.9 mAh/g/cycle). In a rough way, a sample with a smaller first-discharge capacity has a smaller capacity deterioration rate.

The curves of the voltage vs. x in $Li_xNi_{0.7}Co_{0.3}O_2$ at a current density of 200 μA/cm^2 for the first charge–discharge of $LiNi_{0.7}Co_{0.3}O_2$ in Fig. 5 show that, compared with the quantity of the deintercalated Li ions by the first charging, that of the intercalated Li ions by the first discharging is a little smaller. During the first charging, Li ions deintercalate not only from stable 3b sites but also from unstable 3b sites. The destruction of the unstable 3b sites, after deintercalation from unstable 3b sites, is thought to lead to smaller quantity of the Li ions intercalated by the first discharging than that of the Li ions deintercalated by the first charging.

In the curves of voltage vs. x in $Li_xNi_{0.7}Co_{0.3}O_2$ at a current density of 200 μA/cm^2 for the first charge-discharge of $LiNi_{0.7}Co_{0.3}O_2$ synthesized at 850 °C from Li_2CO_3, NiO, and Co_3O_4 shown in Fig. 5(a), the charge–discharge curves exhibit quite long plateaus, where two phases co-exist [41]. During charging and discharging, $LiNiO_2$ goes reportedly through three or four phase transitions [39,42,43]. Song et al. [43] reported that $-dx/|dV|$ vs. V curves of $LiNi_{1-y}Ti_yO_2$ (y=0.012 and 0.025) for charging and discharging showed four peaks, revealing four phase transitions from hexagonal structure (H1) to monoclinic structure (M), from M to hexagonal structure (H2), from H2 to hexagonal structure (H2)+hexagonal structure (H3), and from H2+H3 to H3, or vice versa.

4. Conclusions

Cathode active materials with a composition of $LiNi_{0.7}Co_{0.3}O_2$ were synthesized by a solid-state reaction method at 850 °C using Li_2CO_3, NiO or $NiCO_3$, and Co_3O_4 or $CoCO_3$ as the sources of Li, Ni, and Co, respectively. The electrochemical properties of the synthesized samples were then investigated. The $LiNi_{0.7}Co_{0.3}O_2$ sample synthesized from Li_2CO_3, NiO, and Co_3O_4 had the largest first discharge capacity (127 mAh/g), with a discharge capacity deterioration rate of 2.9 mAh/g/cycle. This sample had the largest particles with quite flat surfaces. The curves of the voltage vs. x in $Li_xNi_{0.7}Co_{0.3}O_2$ for the first charge-discharge of $LiNi_{0.7}Co_{0.3}O_2$ showed that after deintercalation from unstable 3b sites, the unstable 3b sites will be destroyed, leading to a smaller quantity of the Li ions intercalated by the first discharging than that of the Li ions deintercalated by the first charging. In a rough way, a sample with a smaller first-discharge capacity has a smaller capacity deterioration rate.

References

[1] K. Ozawa, Lithium-ion rechargeable batteries with $LiCoO_2$ and carbon electrodes: the $LiCoO_2$/C system, Solid State Ionics 69 (1994) 212–221.
[2] R. Alcántara, P. Lavela, J.L. Tirado, R. Stoyanova, E. Zhecheva, Structure and electrochemical properties of boron-doped $LiCoO_2$, Journal of Solid State Chemistry 134 (1997) 265–273.
[3] Z.S. Peng, C.R. Wan, C.Y. Jiang, Synthesis by sol–gel process and characterization of $LiCoO_2$ cathode materials, Journal of Power Sources 72 (1998) 215–220.
[4] W.D. Yang, C.Y. Hsieh, H.J. Chuang, Y.S. Chen, Preparation and characterization of nanometric-sized $LiCoO_2$ cathode materials for lithium batteries by a novel sol–gel method, Ceramics International 36 (1) (2010) 135–140.
[5] S.K. Kim, D.H. Yang, J.S. Sohn, Y.C. Jung, Resynthesis of $LiCo_{1-x}Mn_xO_2$ as a cathode material for lithium secondary batteries, Metals and Materials International 18 (2) (2012) 321–326.
[6] J.R. Dahn, U. von Sacken, C.A. Michal, Structure and electrochemistry of $Li_{1\pm y}NiO_2$ and a new Li_2NiO_2 phase with the $Ni(OH)_2$ structure, Solid State Ionics 44 (1990) 87–97.
[7] J.R. Dahn, U. von Sacken, M.W. Juzkow, H. Al-Janaby, Rechargeable $LiNiO_2$/carbon cells, Journal of the Electrochemical Society 138 (1991) 2207–2212.
[8] B.H. Kim, J.H. Kim, I.H. Kwon, M.Y. Song, Electrochemical properties of $LiNiO_2$ cathode material synthesized by the emulsion method, Ceramics International 33 (2007) 837–841.
[9] H.U. Kim, D.R. Mumm, H.R. Park, M.Y. Song, Synthesis by a simple combustion method and electrochemical properties of $LiCo_{1/3}Ni_{1/3}Mn_{1/3}O_2$, Electronic Materials Letters 6 (3) (2010) 91–95.
[10] S.H. Ju, J.H. Kim, Y.C. Kang, Electrochemical properties of $LiNi_{0.8}Co_{0.2-x}Al_xO_2$ ($0 \le x \le 0.1$) cathode particles prepared by spray pyrolysis from the spray solutions with and without organic additives, Metals and Materials International 16 (2) (2010) 299–303.
[11] S.N. Kwon, J.H. Song, D.R. Mumm, Effects of cathode fabrication conditions and cycling on the electrochemical performance of $LiNiO_2$ synthesized by combustion and calcination, Ceramics International 37 (5) (2011) 1543–1548.

[12] M.Y. Song, C.K. Park, H.R. Park, D.R. Mumm, Variations in the electrochemical properties of metallic elements-substituted $LiNiO_2$ cathodes with preparation and cathode fabrication conditions, Electronic Materials Letters 8 (1) (2012) 37–42.
[13] M.Y. Song, D.R. Mumm, C.K. Park, H.R. Park, Cycling performances of $LiNi_{1-y}M_yO_2$ (M=Ni, Ga, Al and/or Ti) synthesized by wet milling and solid-state method, Metals and Materials International 18 (3) (2012) 465–472.
[14] J.M. Tarascon, E. Wang, F.K. Shokoohi, W.R. Mckinnon, S. Colson, The spinel phase of $LiMn_2O_4$ as a cathode in secondary lithium cells, Journal of the Electrochemical Society 138 (1991) 2859–2864.
[15] A.R. Armstrong, P.G. Bruce, Synthesis of layered $LiMnO_2$ as an electrode for rechargeable lithium batteries, Letters in Nature 381 (1996) 499–500.
[16] M.Y. Song, D.S. Ahn, On the capacity deterioration of Spinel phase $LiMn_2O_4$ with cycling around 4V, Solid State Ionics 112 (1998) 21–24.
[17] M.Y. Song, D.S. Ahn, H.R. Park, Capacity fading of spinel phase $LiMn_2O_4$ with cycling, Journal of Power Sources 83 (1999) 57–60.
[18] D.S. Ahn, M.Y. Song, Variations of the electrochemica properties of $LiMn_2O_4$ with synthesis conditions, Journal of the Electrochemical Society 147 (3) (2000) 874–879.
[19] H.J. Guo, Q.H. Li, X.H. Li, Z.X. Wang, W.J. Peng, Novel synthesis of $LiMn_2O_4$ with large tap density by oxidation of manganese powder, Energy Conversion and Management 52 (4) (2011) 2009–2014.
[20] C. Wan, M. Cheng, D. Wu, Synthesis of spherical spinel $LiMn_2O_4$ with commercial manganese carbonate, Powder Technology 210 (1) (2011) 47–51.
[21] J.W. Park, J.H. Yu, K.W. Kim, H.S. Ryu, J.H. Ahn, C.S. Jin, K.H. Shin, Y.C. Kim, H.J. Ahn, Surface morphology changes of lithium/sulfur battery using multi-walled carbon nanotube added sulfur electrode during cyclings, Korean Journal of Metals and Materials 49 (2) (2011) 174–179.
[22] Y. Nishida, K. Nakane, T. Satoh, Synthesis and properties of gallium-doped $LiNiO_2$ as the cathode material for lithium secondary batteries, Journal of Power Sources 68 (1997) 561–564.
[23] P. Barboux, J.M. Tarascon, F.K. Shokoohi, The use of acetates as precursors for the low-temperature synthesis of $LiMn_2O_4$ and $LiCoO_2$ intercalation compounds, Journal of Solid State Chemistry 94 (1991) 185–196.
[24] J. Morales, C. Perez-Vicente, J.L. Tirado, Cation distribution and chemical deintercalation of $Li_{1-x}Ni_{1+x}O_2$, Materials Research Bulletin 25 (1990) 623–630.
[25] B.J. Neudecker, R.A. Zuhr, B.S. Kwak, J.B. Bates, J.D. Robertson, Lithium manganese nickel oxides $Li_x(Mn_yNi_{1-y})_{2-x}O_2$, Journal of the Electrochemical Society 145 (1998) 4148–4157.
[26] A. Rougier, I. Saadoune, P. Gravereau, P. Willmann, C. Delmas, Effect of cobalt substitution on cationic distribution in $LiNi_{1-y}Co_yO_2$ electrode materials, Solid State Ionics 90 (1996) 83–90.
[27] C. Delmas, I. Saadoune, Electrochemical and physical properties of the $Li_xNi_{1-y}Co_yO_2$ phases, Solid State Ionics 53–56 (1992) 370–375.
[28] E. Zhecheva, R. Stoyanova, Stabilization of the layered crystal structure of $LiNiO_2$ by Co-substitution, Solid State Ionics 66 (1993) 143–149.
[29] C. Delmas, I. Saadoune, A. Rougier, The cycling properties of the $Li_xNi_{1-y}Co_yO_2$ electrode, Journal of Power Sources 43–44 (1993) 595–602.
[30] A. Ueda, T. Ohzuku, Solid-state redox reactions of $LiNi_{1/2}Co_{1/2}O_2$ ($R\bar{3}m$) for 4 V secondary lithium cells, Journal of the Electrochemical Society 141 (1994) 2010–2014.
[31] M. Menetrier, A. Rougier, C. Delmas, Cobalt segregation in the $LiNi_{1-y}Co_yO_2$ solid solution: a preliminary ^7Li NMR study, Solid State Communications 90 (1994) 439–442.
[32] R. Alcantara, J. Morales, J.L. Tirado, R. Stoyanova, E. Zhecheva, Structure and electrochemical properties of $Li_{1-x}(Ni_yCo_{1-y})_{1+x}O_2$ Effect of chemical delithiation at 0 °C, Journal of the Electrochemical Society 142 (1995) 3997–4005.
[33] B. Banov, J. Bourilkov, M. Mladenov, Cobalt stabilized layered lithium-nickel oxides, cathodes in lithium rechargeable cells, Journal of Power Sources 54 (1995) 268–270.
[34] Y.M. Choi, S.I. Pyun, S.I. Moon, Effects of cation mixing on the electrochemical lithium intercalation reaction into porous $Li_{1-\delta}Ni_{1-y}Co_yO_2$ electrodes, Solid State Ionics 89 (1996) 43–52.
[35] S.J. Lee, J.K. Lee, D.W. Kim, H.K. Baik, S.M. Lee, Fabrication of thin film $LiCo_{0.5}Ni_{0.5}O_2$ cathode for Li rechargeable microbattery, Journal of the Electrochemical Society 143 (1996) L268–L270.
[36] D. Caurant, N. Baffier, B. Garcia, J.P. Pereira-Ramos, Synthesis by a soft chemistry route and characterization of $LiNi_xCo_{1-x}O_2$ ($0 \le x \le 1$) cathode materials, Solid State Ionics 91 (1996) 45–54.
[37] K. Amine, H. Yasuda, Y. Fujita, New process for low temperature preparation of $LiNi_{1-x}Co_xO_2$ Cathode material for lithium cells, Annales de Chimie: Science des Matériaux 23 (1998) 37–42.
[38] C.C. Chang, N. Scarr, P.N. Kumta, Synthesis and electrochemical characterization of $LiMO_2$ (M=Ni, $Ni_{0.75}Co_{0.25}$) for rechargeable lithium ion batteries, Solid State Ionics 112 (1998) 329–344.
[39] T. Ohzuku, A. Ueda, M. Nagayama, Electrochemistry and structural chemistry of $LiNiO_2$ ($R\bar{3}m$) for 4 V secondary lithium cells, Journal of the Electrochemical Society 140 (1993) 1862–1870.
[40] M.Y. Song, H. Rim, E. Bang, Electrochemical properties of cathode materials $LiNi_{1-y}Co_yO_2$ synthesized using various starting materials, Journal of Applied Electrochemistry 34 (2004) 383–389.
[41] W. Li, J.N. Reimers, J.R. Dahn, In situ X-ray diffraction and electrochemical studies of $Li_{1-x}NiO_2$, Solid State Ionics 67 (1993) 123–130.
[42] H. Arai, S. Okada, H. Ohtsuka, M. Ichimura, J. Yamaki, Characterization and cathode performance of $Li_{1-x}Ni_{1+x}O_2$ prepared with the excess lithium method, Solid State Ionics 80 (1995) 261–269.
[43] M.Y. Song, D.S. Lee, H.R. Park, Electrochemical properties of $LiNi_{1-y}Ti_yO_2$ and $LiNi_{0.975}M_{0.025}O_2$ (M=Zn, Al, and Ti) synthesized by the solid-state reaction method, Materials Research Bulletin 47 (2012) 1021–1027.